STATUS OF THE KEK PS MAIN RING

KEK Accelerator Main Ring Group
(presented by Y. Kimura)
National Laboratory for High Energy Physics

The KEK proton synchrotron consists of four stages of accelerators as illustrated in Fig.1. The beam from the 20 MeV linac is accelerated to 500 MeV in the booster synchrotron and transferred to the main ring. The linac and the booster are operated at 20 Hz, while one cycle of the main ring takes about 2 sec. The main ring has a flat injection field porch lasting about 0.7 sec. and starts the acceleration after accepting nine successive booster pulses. The main design parameters of the accelerators are summarized in Table 1.

After succeeding in accelerating protons to the design energy 12 GeV in March 1976, we have steadily been improving the performances of the main ring. Figure 2 illustrates how the main ring intensity has been increased in these two years. Present intensity of $\sim 1.8 \times 10^{12}$ ppp is already very close to the design value of 2×10^{12} ppp. Nevertheless, many problems still reamin outstanding in the main ring. Figure 3 shows a typical example of beam current

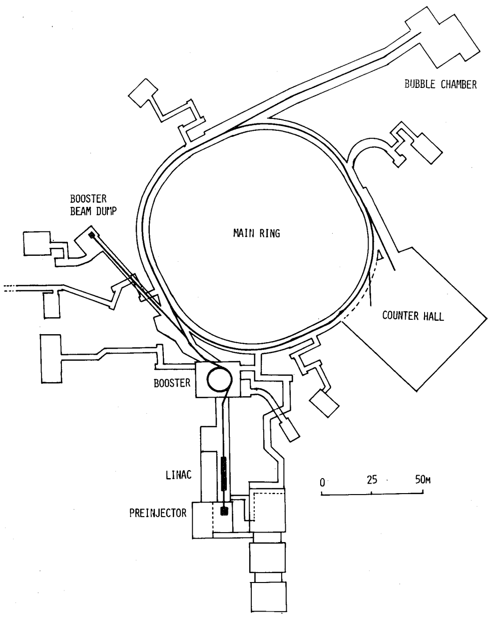

Fig.1 Layout of the KEK accelerators.

PARAMETERS OF KEK ACCELERATOR

I. MAIN RING	
KINETIC ENERGY	12 GEV (8 GEV)
INTENSITY (SPACE CHARGE LIMIT)	$\geq 2\times10^{12}$ (1×10^{13}) PPP
TYPE	SEPARATED-FUNCTION
FOCUSING ORDER	FODO
AVERAGE RADIUS	54 M
NUMBER OF SPERPERIOD	4
NUMBER OF BETATRON OSCILLATIONS	7.25
MAXIMUM BENDING FIELD	17.5 KG
INJECTION ENERGY	0.5 GEV
REPETITION RATE	0.5 HZ
II. BOOSTER	
KINETIC ENERGY	500 MEV
INTENSITY (SPACE CHARGE LIMIT)	6×10^{11} (3×10^{12}) PPP
TYPE	COMBINED -FUNCTION
FOCUSING ORDER	FDFO
AVERAGE RADIUS	6.0 M
NUMBER OF CELLS	8
NUMBER OF BETATRON OSCILLATIONS	2.25
MAXIMUM MAGNETIC FIELD	11 KG
REPETITION RATE	20 HZ
III. LINAC	
ENERGY	20 MEV
TYPE	SINGLE TANK D-T LINAC
CAVITY LENGTH	15.5 M
NUMBER OF CELLS	90
PEAK CURRENT	100 MA
REPETITION RATE	20 HZ
PREINJECTOR	750 KV COCKCROFT-WALTON

Table 1

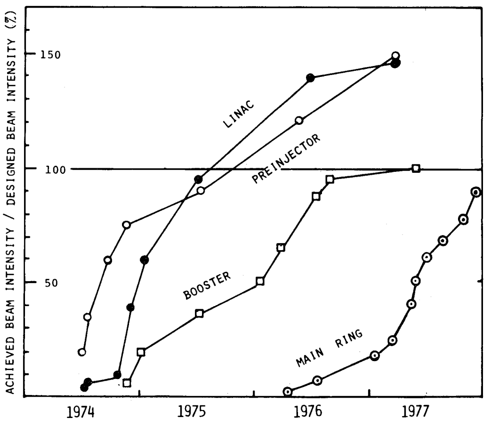

Fig.2 Growth of the beam intensity achieved in operating the machines for the last three years.

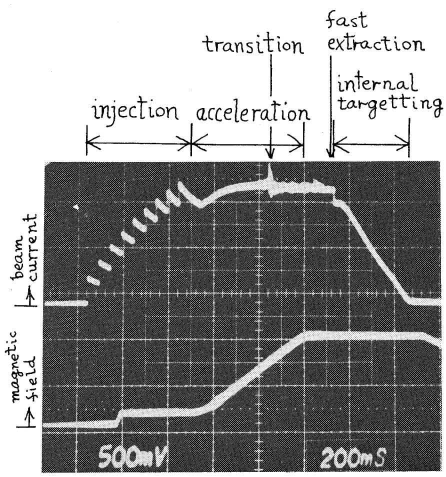

Fig.3 Beam current in the main ring through one magnet cycle.

in the main ring through one magnet cycle. Considerable amounts of beam losses are observable during the injection period of about 0.5 sec. Number of protons which survive in the ring at the start of the acceleration are only about 40 $\sim$ 50 % of what are successively transferred from the booster. To improve the beam transmission, behaviours of the beam after injection have extensively been studied by varying various parameters of the main ring. Horizontal and vertical tune (ν_H, ν_V) which gave a maximum transmission were searched for in the tune diagram region of $5 < \nu_H, \nu_V < 8$. The best tunes were determined to be $\nu_H = 7.12$ and $\nu_V = 6.18$. Figure 4 shows the transmission factor measured at the injection porch (relative scale) as a function of (ν_H, ν_V). As the main ring has non zero chromaticity unless corrected, the momentum spread of the injected beam ($|\Delta p/p| \sim 3 \times 10^{-3}$) causes an undesirable tune spread ($|\Delta\nu_H| \sim 0.05$, $|\Delta\nu_V| \sim 0.02$). Then, the chromaticity has been reduced to zero by using 16 auxiliary sextupole magnets distributed around the ring (Fig.5). This correction was very effective and almost doubled the transmission efficiency. However, even after the chromaticity has been corrected, there exist considerable amounts of tune spread. Though what causes this effect has not been fixed, this tune spread was found to be one which depends on transverse oscillation amplitudes. The closed orbit distortions are corrected by adjusting steering dipoles which are located next to every quadrupole of the main ring lattice. The correction in the vertical plane is very

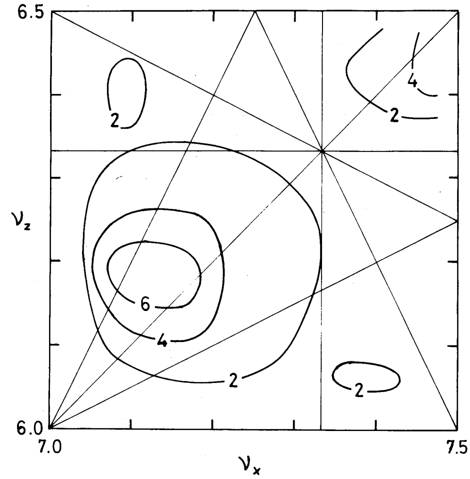

Fig.4 Beam transmission efficiency at the injection (relative scale) as a function of (ν_H, ν_V).

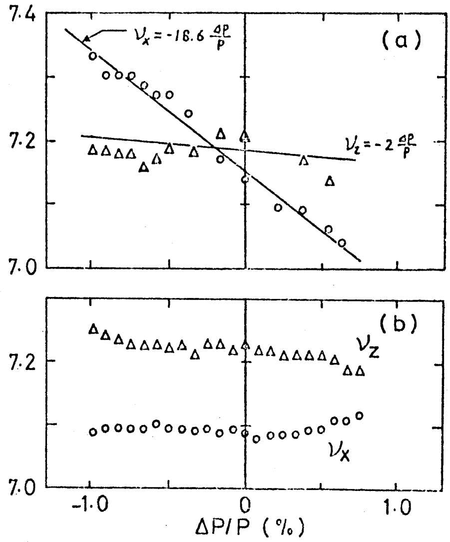

Fig.5 Chromaticity of the main ring. (a) and (b) show values measured before and after the correction, respectively.

crucial to improve the transmission, and an insufficient vertical useful aperture of the ring is thought to be a main cause of the beam loss during the injection period. What is worse, the vertical emittance of the booster beam was observed to blow up by more than 100 % due to space charge effects during the acceleration. Therefore, the present efforts to improve the beam transmission at the injection are concentrated in adjusting the closed orbit as finely as possible and in looking for the root cause which makes the useful apertures of the ring considerably smaller than the design values.

About 10 ∿ 20 % of the beam accelerated is lost when crossing the transition energy. Though the beam loss happens at or after the transition, we have observed that what triggers the loss is a bunch oscillation which starts far before the beam reaches the transition. Figure 6(a) shows a typical example of the beam loss at the transition with accompanying a radial beam oscillation, while Fig.6(b) is an example in which the beam crosses the transition without loss and shows no radial oscillations before the transition. The reason of this phenomenon is still under investigation.

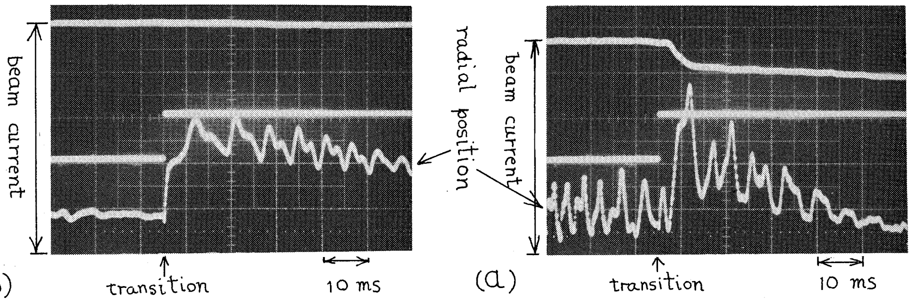

Fig.6 Correlation between the beam loss at the transition and the radial oscillation of the beam existing before the transition.

Since May 1977, the main ring beam has been supplied for physics experiments. About 10 % of the beam is extracted to the bubble chamber beam line at the beginning of the magnetic field flat top, and remaining protons are slowly brought onto the internal target to produce a spill of secondary particles lasting about 0.4 sec. The fast beam extraction for the bubble chamber is performed by shaving out a part of the beam kicked into the electrostatic wire septum (50 μm thick) inflector. We have started the tests of slow beam extraction for electronic counter experiments last November. Half-integral resonant extraction is employed at a horizontal tune of $\nu_H = 7.5$. After bringing ν_H close to the half-integer by the main ring quadrupole, the stop-band is created by exciting two auxiliary quadrupoles to initiate the extraction. An octupole magnet as a non-linear perturbing element provides necessary growth rate of the betatron oscillation amplitude. By adjusting the extraction elements, quadrupoles, octupoles, bump magnets and extraction septa, we have obtained extraction efficiency of 80 ∿ 90 %. Figures 7(a), (b), and (c) show typical spill of the fast extracted, the internal target, and the slow extracted beam, respectively.

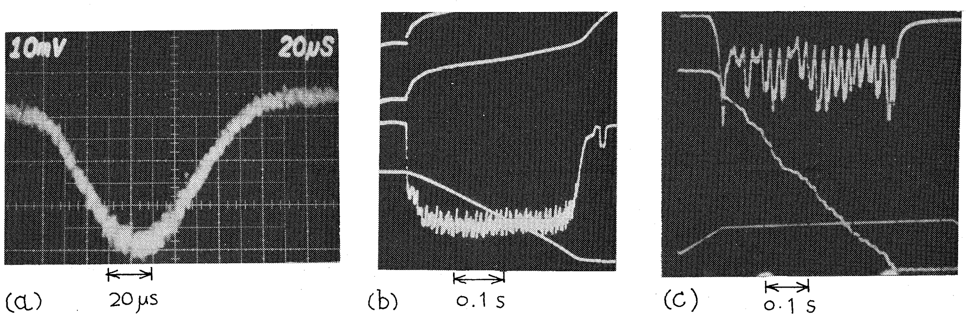

Fig.7 Typical spill of (a) the fast extracted, (b) the internal target, and (c) the slow extracted beam.